Wall Thickness Optimization of GRP Process Pipes

Tony Lallinaho

Degree Thesis

Plastteknik

2017

DEGREE THESIS	
Arcada	
Degree Programme:	Plastteknik
Identification number:	
Author:	Tony Lallinaho
Title:	Wall Thickness Optimization of GRP Process Pipes
Supervisor (Arcada):	Rene Herrmann
Commissioned by:	River Plast Oy

Abstract:
River Plast Oy manufactures high-pressure glass fiber reinforced process pipes by filament winding technology. The company wants to minimize the wall thickness of their pipes with respect to the nominal pressure. According to standards, the pipe PN10 DN300 has to withstand six times the nominal pressure 10 bar, i.e. 60 bar without failing. Also, the minimum wall thickness allowed for the pipe is 5.0 mm. The pipe consists of three functional layers: a corrosion barrier, a structural layer and a surface layer. There is no model for the strength calculations – only for the moduli. If a maximal allowable strain is assumed, the required moduli can be calculated. Thickness minimizing strategy for pressure loaded pipes is that the strains in the hoop and axial directions are equal, indicating that the hoop modulus is approximately double the axial modulus. Three different material combinations were selected to test the calculation model. It was found out that the suggested combinations gave nonoptimal moduli and therefore unequal strains: The first combination resulted in 24.5 GPa and 10.3 GPa in the hoop and axial directions, respectively. The second combination gave 25.3 GPa and 11.2 GPa and the third 28.2 GPa and 8.3 GPa, respectively. Each combination resulted in different wall thicknesses: 5.3 mm, 4.9 mm and 4.9 mm, respectively. There are limitations in the calculation model. It neglects the mass and the ends of the pipe, where the stress-strain behavior is different so it considers the middle section only. Also, it assumes the laminate to be balanced and having a constant thickness, which in terms gives higher moduli than if the laminate had variation within the layers. It was found out that there are variations within the layers, hence it will affect the laminate performance. To fix these variations, suggestions were given to improve the winding strategy. Regarding further studies, it was recommended to inspect the displacement of the pipe at different points around the circumference as a function of pressure.

Keywords:	Process pipe, glass fiber, laminate, filament winding, wall thickness, optimization, dimensioning
Number of pages:	43
Language:	English
Date of acceptance:	

EXAMENSARBETE	
Arcada	
Utbildning:	Plastteknik
Identifikationsnummer:	
Författare:	Tony Lallinaho
Arbetets namn:	Optimering av väggtjockleken på glasfiberarmerade processrör
Handledare:	Rene Herrmann
Uppdragsgivare:	River Plast Oy

Sammandrag:
River Plast Oy tillverkar tryckbelastade processrör med filamentlindningsteknik. Bolaget vill minimera rörens väggtjocklek med avseende på nominellt tryck. Enligt standarder bör rörmodellen PN10 DN300 hålla sex gånger så mycket som det nominella trycket 10 bar, det vill säga 60 bar, utan att brytas. Den minimala väggtjockleken för röret är 5.0 mm. Röret består av tre olika lager: korrosionsbarriären, det förstärkande lagret och ytlagret. Det finns ingen modell för hållfasthetsberäkning – bara för modulberäkning. Om en maximal, tillåten brottgräns är given kan man räkna ut de elasticitetsmoduler som krävs för röret. Strategin för att uppnå den minimala väggtjockleken är att töjningarna i båda huvudriktningarna är lika, vilket innebär att modulen i radialriktningen är ungefär dubbelt så stor som modulen i axialriktningen. Tre olika materialkombinationer förslogs för att testa kalkylmodellen. Det visade sig att modulförhållandena blev inte optimala: den första kombinationen gav 24.5 GPa i radial- och 10.3 GPa i axialriktningen. Det andra och tredje förslaget gav 25.3 GPa och 11.2 GPa samt 28.2 GPa och 8.3 GPa i respektive riktningar. Väggtjocklekarna för varsin kombination blev 5.3 mm, 4.9 mm och 4.9 mm, respektive. Det finns brister i kalkylmodellen. Den antar att röret har ingen massa och tar i beaktande endast mittsektionen på röret, såvida ignorerar ändorna där förhållandet mellan spänning och töjning är annorlunda. Enligt modellen är laminatet balanserat och har konstant väggtjocklek. Eventuella tjockleksvariationer mellan och inuti skikten i laminatet skulle inverka negativt på modulerna. Av ett provrör framgick det att variationer existerar mellan tjockleken. För att minimera variationerna gavs förlsag för utveckling av lindningsstrategin. Rekommendationer för vidare studier skulle innebära att undersöka rörets förskjutning vid olika punkter kring omkretsen som funktion av tryckbelastning.

Nyckelord:	Processrör, glasfiber, laminat, filamentlindning, väggtjocklek, optimering, dimensionering
Sidantal:	43
Språk:	Engelska
Datum för godkännande:	

CONTENTS

Figures

Tables

List of Symbols

α = arbitrary angle alfa

θ = arbitrary angle theta

σ = tensile stress

ε = tensile strain

τ = shear stress

γ = shear strain

List of Abbreviations

A = extensional stiffness matrix

B = coupling stiffness matrix

D = bending stiffness matrix

DN = diameter nominal

E = elastic modulus

f = fiber volume fraction

G = shear modulus

GRP = glass fiber reinforced plastics

N_m = rotational speed of mandrel

N_s = speed of carriage

p = inner pressure

PN = pressure nominal

Q = lamina stiffness matrix

R = inner radius

S = lamina compliance matrix

t = thickness

Tex = mass in grams per 1000 meters

UD = unidirectional

v = Poisson’s ratio

FOREWORD

I want to thank Saku Miikki and Hannu Viitikko from River Plast Oy for a challenging thesis topic. Then I also want to thank lecturer Rene Herrmann for guidance and for helping me to understand the mechanics of composite materials. Special thanks to Erland Nyroth, who helped me with the machining and Lev Lebedev, who helped me with the microscope. I also want to thank Mika Hurri from Ahlstrom Glassfibre Oy for sharing alternatives regarding glass fiber materials.

1 INTRODUCTION

Industries have constantly to develop their operations to make their products more competitive. These operations consider e.g. the manufacturing processes and selecting the best raw materials available with respect to the quality-price ratio. When it comes to product development, it is also conventional to consider the demands and the limits of the design before going any further. In this thesis, the strength properties of glass fiber reinforced process pipes are investigated using the classic lamina theory and compared to an existing calculation model. However, this model includes simplified assumptions which in terms mislead one to consider a perfect laminate, i.e. there are some issues that affect the laminate properties negatively which the calculation model does not take in to account.

1.1 Background

River Plast Oy produces GRP (Glass Fiber Reinforced Plastics) pipes by a method called filament winding. Products manufactured by this method are to fulfill specifications of different standards. These standards define e.g. the compatible materials that can be used for the design purpose. They also specify the design and dimensioning principles and testing methods – i.e. standards set frames for all the operations and therefore cannot be neglected. In this case, a pipe of model PN10 DN300 is to withstand six times the nominal pressure 10 bar, yielding 60 bar without failing. By using all of this as a starting point, the company wants to optimize the strength of their pipes and minimizing the wall thickness with respect to the nominal pressure. One of the key points is to select the best combination of two variables – axial and hoop reinforcements – as the raw materials for the winding process. The reinforcements to be selected might be in form of roving, unidirectional or multiaxial stiches or woven fabrics. Regardless the choice, they all should be compatible with the resin so that they get wetted out. In this work, the resin considered is vinyl ester. Selecting the best combination requires comparative combinations. Hence, three different combinations are suggested and analyzed by strength calculations. These suggestions could act as good references to further work for selecting and verifying the final combinations. The tool used for the calculations is based on a calculation model,

which in turn includes shortages and therefore can't be fully relied on. In this thesis, the shortages are identified and suggestions are made for improving the winding strategy.

1.2 Objectives

The research questions of this thesis are as follows:

- Implement a calculation tool for dimensioning a pressure vessel
- Define thickness minimizing boundaries
- Identify shortenings in the calculation model
- Suggest design improvements to winding strategy of PN10 DN300 pipes

2 LITERATURE REVIEW

This chapter deals with the fundamentals of the filament winding technology, the practical demands and other aspects that is to be taken into consideration. The classic lamina theory is used as a basis prior to the strength calculations of the pipe in chapter 3.

2.1 Filament Winding

2.1.1 Principle

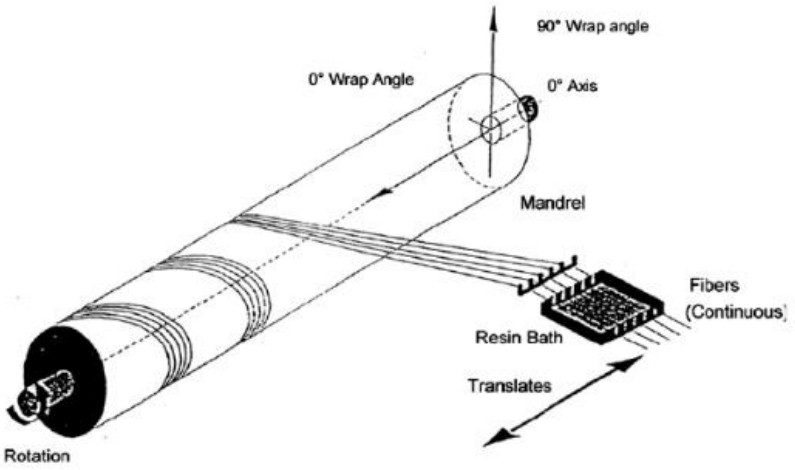

Figure 1: Schematic of filament winding process (Rafiee, 2013, pp. 257-267)

Filament winding is a process where a winding machine is used to wrap resin impregnated, reinforcing fibers on a rotating mandrel specimen (Mutasher, et al., 2012). The continuous reinforcements form a helical pattern along the mandrel forming a lightweight and strong cylindrical laminate. Modern machines operate under the control of software such as CADWIND™, EasyWinder™ and FiberGrafiX™, to name a few. The technology has been recognized cost effective to manufacture composite products with remarkable properties and is mostly used in manufacturing corrosion resistant pipes and vessels (Saarela, et al., 2003).

2.1.2 Machine Properties

Product properties can be varied by adjusting the winding pattern. These winding patterns are typically hoop winding, helical winding and polar winding. According to Mutasher et al., the fibers will pass through a resin bath in order to wet out and fed onto the mandrel. The bath also includes guiding rollers and eyes or similar in order to smear off excess resin from the wetted fibers. Subsequently, the wetted fibers are lead through a carriage onto the mandrel. By determining the amount of fiber bundles, the width of the winded band can be defined. In the machine design presented by Mutasher et al., by moving linearly on a lead screw which forms a rotary-to-linear motion transmission, the carriage is moved back and forth along the length of the mandrel. By coordinating the movement of the carriage and the mandrel the winding angle can be desired (Saarela, et al., 2003). There is a relationship between the winding angle and the rotational speed of the mandrel as well as the linear speed of the carriage. It leads:

$$\tan\theta = \frac{r2\pi N_m}{LN_s} \qquad 2.1$$

where
$\tan\theta$ = winding angle (deg)
r = winding radius (mm)
N_m = rotational speed of the mandrel (rpm)
N_s = speed of carriage (mm/min)
L = the screw lead (mm/rev) (Mutasher, et al., 2012)

Mutasher et al., names all of the previous as the delivery unit. Hence, the delivery unit delivers the wetted fibers onto the rotating mandrel – the rotary unit, where the wetted fibers are let to be cured. A schematic of the process is presented in *Figure 1*. To control and keep the fiber tension constant, the fibers are passing roller guides, comb or scissor bar. Keeping the fiber tension constant throughout the whole lamination process is one of the essential properties of the winding machine (Saarela, et al., 2003). Other important properties are the accuracy of steering of the winding, arrangement of mold handling and repeatability of layers as well as minimizing the waste of material at the ends of the pipe

where the winding direction changes. Saarela et al. state that there is no technical upper limit of filament wound product sizes. Nowadays, the biggest horizontally wound products are 6-7 meters in diameter, whereas vertically wound product diameters exceed 20 meters.

2.1.3 Raw Materials

Product properties can also be varied by selecting a combination of reinforcements and resin system with predetermined mechanical and physical properties. Common reinforcement materials found from the industry are E-glass, S-glass, carbon fiber and aramid fibers (Mutasher, et al., 2012). The corrosion resistance of plastic composites originates from the resin properties (Saarela, et al., 2003). These resins provide good chemical and weather resistance. Polyesters are the most common resin types, but in special cases also epoxy and phenolic resins are used. It is important that the viscosity of the resin is low enough to enable fast wetting and long working time. Usually, resin systems with long working times require elevated temperatures for curing. The product can be heated by using infra-red lamps at the mold or alternatively, it can be placed in an oven. The reinforcements are to large extent glass fiber roving, but also chopped strand mats, non-woven veils and woven fabrics are commonly used. The latter are wound onto the mold mainly as a band with a certain width. Furthermore, Saarela et al. explain that they can be applied dry between the roving layers or wetted in the resin bath before winding. Products based on thermoset resin can also be wound of prepregs. Prepregs are semi-finished products where the fibers are pre-impregnated with the resin, i.e. including all the ingredients required for curing. Benefits of prepregs in filament winding are that there is no need of external resin bath and simultaneously, working become cleaner and the products of higher quality. Also, thermoplastics can be applied in filament winding, according to Saarela et al. Here the prepreg band is first heated to its melting point locally on the mold surface and subsequently pressed onto the layer underneath.

2.1.4 Product Properties

The mechanical properties of the filament wound products are superior since the reinforcements are continuous and directional. Additionally, it is possible to achieve high

fiber volume fraction so that the properties can be as good as obtained by prepreg lamination or autoclave curing. Winding technology also enables the use of fibers with required reinforcing directions prior to the product demands, even when concerning with products with complex geometry. Generally, the geometry of all products should be designed in the way that the fibers will continuously be in tensile loading during the winding process. Even after successful winding the products can be post processed separately e.g. with different compression methods. From a financial point of view, the reinforcing in filament winding is in its cheapest form and the productivity is high. Simultaneously, the properties and the price make the final product very competitive. (Saarela, et al., 2003). GRP pipes provide high mechanical strength with outstanding fatigue resistance and high impact resistance, high temperature resistance and 200 times better thermal insulation than steel. The inner surface is smooth with low coefficient of friction, which in turn results in low pumping costs. Additionally, GRP pipes can be easily upgraded with different additives, e.g. for improved abrasion resistance, electrical conductivity and fire resistance. Compared to steel, GRP pipes are cost-effective i.e. they provide reduced installation and maintenance costs as well as longer service life and less complex support structures. The pipe is light weight making the handling easy and installation time faster (Plasticon Composites, 2017).

2.1.5 Wall Construction

GRP pipes are built up of several laminate stacks, all providing their own functionalities. The wall system is built up of three layers – the liner, structural layer and top coat, as shown in *Figure 2* below. In filament winding processes, the inner layer is called a liner and consists of a layer of pure resin followed by gelcoat (Plasticon Composites, 2017) resin-impregnated surface veils and chopped strand mats of glass fiber (Rafiee, 2013). The thickness of the liner varies from 0.5 to 6.3 mm and it works as a chemical barrier protecting the structural layers from the transmitted, corrosive fluids and gases. On the liner, the structural layer is wound using resin impregnated E-glass direct roving, but also woven fabrics are utilized (Saarela, et al., 2003). It provides high mechanical strength and resistance to hoop and axial loads (Plasticon Composites, 2017). The top layer or top coat includes a surface veil, also resin impregnated. This layer gives the product a smooth outer surface and protects it from all kinds of weather, UV radiation and chemicals.

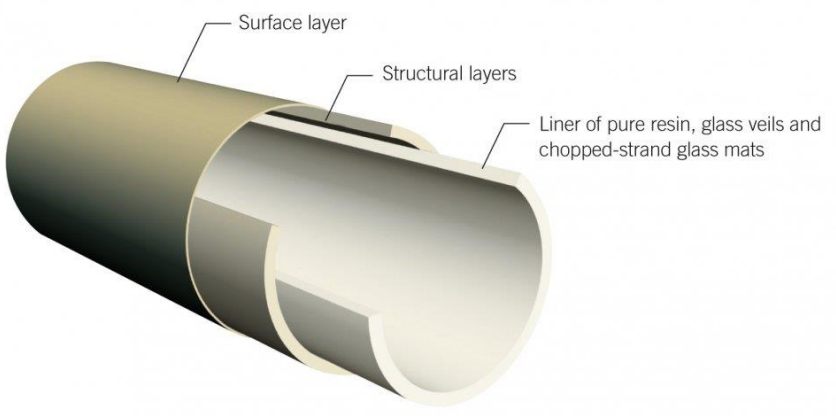

Figure 2: Structural illustration of a typical GRP pipe (Plasticon Composites, 2017)

2.2 Overview of Analysis Fundamentals

2.2.1 Essentials

When a reinforcement is mixed with a resin matrix and let to be cured, the resultant is a single layer called a lamina (Prof. Dr. Tapavicza, 2010). When it comes to design of fiber reinforced plastic (FRP) components, it is to be taken into consideration that the components are anisotropic and represents inhomogeneous characteristics (Verein Deutscher Ingenieure, 2006). Anisotropy means that the properties are not the same in all directions and the inhomogeneity refers to the layers and interfaces of the fiber reinforcement and the matrix. According to VDI, the mechanical properties of the fibers and the matrix are very different which leads to local variations in stress states in the laminate, especially in a single lamina. Analyzing individual fibers surrounded by the resin matrix is called the study of micromechanics. From an engineering point of view, a laminate is examined in a larger scale. This level is defined as macromechanics. Here the inhomogeneity is neglected, because the properties of the fibers and the matrix are put together and analyzed one lamina at a time. VDI means that when building up the laminate from individual laminae, each of these layers can be analyzed and dimensioned separately one at a time. For the analysis, following lamina input variables are required:

- Fiber content
- Lamina thickness

- Type and orientation of reinforcement
- Data for stress-strain behavior incl. elasticity and strength properties

2.2.2 Structural Dimensioning

There are several starting points that are to be taken into consideration when dealing with structural dimensioning and one of these are the structural criteria. According to one of these criteria, any crazing can't become apparent in a structure. The criteria concern especially pipe and vessel manufacturing in process industries. Another criteria leads that the structure must have – in all operating conditions – a defined minimum safety limit prior to fracture in static short-term loading. The required safety limit depends on the application area of the structure and the reliability of the design allowable. Here the design allowable mean the moduli and strengths in tensile, compression and shear of each layer in the laminate. These are the most important properties and can be analyzed by calculation, e.g. utilizing the classic laminate theory, which is a simple method but requires hard work when dealing with many layers. On the other hand, there are many different software to make the steps easier. However, the classic lamina theory is based on many assumptions and therefore the outcome tells not the whole truth. Because of this, the design allowable should sometimes also be defined in practice by mechanical testing of the laminate selected for the structure. In addition to the design allowable mentioned above, an essential property is also the shear strength between the layers. This is to be taken into consideration if the shear stresses between the layers are significant in the application. (Saarela, et al., 2003)

2.2.3 Failure Modes

When considering the stress leading to failure, the lamina is to be imagined as a homogenous, orthotropic continuum and it has to be drawn a distinction between fracture between the fibers and a fracture of the fibers (Verein Deutscher Ingenieure, 2006). The fracture between the fibers – so called inter-fiber fracture (IFF) should be interpret as a macroscopic crack through the whole thickness of the lamina, which is stopped at the interface to neighboring layers. On the other hand, a fracture of the fibers (FF) deals with

breaking of a big amount of fibers leading to the loss in load bearing capacity in the fiber direction of the affected layer.

2.3 Lamina Analysis

The mechanical properties of this lamina are dependent on the mechanical properties of the reinforcement and the resin, i.e. the combination of these. By knowing the properties of the reinforcement and the resin, new values can be obtained for the lamina. This chapter is guiding through from the determination of properties for a single layer to a full laminate stack, consisting of multiple layers of laminae.

2.3.1 The Elastic Properties of a Single Layer of Unidirectional Fibers

For calculating the elastic properties of a single layer of unidirectional fibers, there are some parameters that should be known (Sutcliffe, et al., 2013). These parameters are the elastic and shear moduli as well as the fiber volume fraction and the Poisson's ratios of the fibers and the resin, respectively. Fiber volume fraction is defined as the volume content of fibers in the total volume of the lamina. The engineering constants are the elastic moduli in direction 1 and 2, the shear modulus in plane and the Poisson's ratios. Hence, the law of mixtures states:

$$E_1 = E_{fiber} f + (1 - f) E_{resin} \tag{2.2}$$

$$\frac{1}{E_2} = \frac{f}{E_{fiber}} + \frac{1 - f}{E_{resin}} \tag{2.3}$$

$$\frac{1}{G_{12}} = \frac{f}{G_{fiber}} + \frac{1 - f}{G_{resin}} \tag{2.4}$$

$$v_{12} = v_{fiber} f + (1 - f) v_{resin} \tag{2.5}$$

$$v_{21} = v_{12} \frac{E_2}{E_1} \tag{2.6}$$

where

$E_{fiber/resin}$ = elastic modulus of fiber/resin

$G_{fiber/resin}$ = shear modulus of fiber/resin

$v_{fiber/resin}$ = Poisson's ratio of fiber/resin

$E_{1/2}$ = elastic modulus in primary/secondary direction

G_{12} = shear modulus in plane prior to direction 1 and 2

$v_{12/21}$ = Poisson's ratios

f = fiber volume fraction

2.3.2 Analysis of a Single Lamina

Once a lamina is produced of unidirectional fibers, three different moduli, e.g. one for each direction, E_1, E_2 and E_3 are obtained (Roylance, 2000). This leads to an orthotropic material because the moduli in direction 1 is bigger than that in the transverse directions 2 and 3. Hence, $E_1 \neq E_2 \neq E_3$. However, Roylance explains that it is common that the properties in directions 2 and 3 – representing the perpendicular plane to direction 1 – can be considered equal, thus $E_2 = E_3$. The lamina is transversely isotropic (Verein Deutscher Ingenieure, 2006). It means that rather than being in a three-dimensional state of stress, the lamina can be assumed to be in a two-dimensional state of stress (Sutcliffe, et al., 2013). An illustration of the directions is presented in *Figure 3* which shows a two layer (= two lamina), unidirectional laminate, where $E_1 \neq E_2 = E_3$.

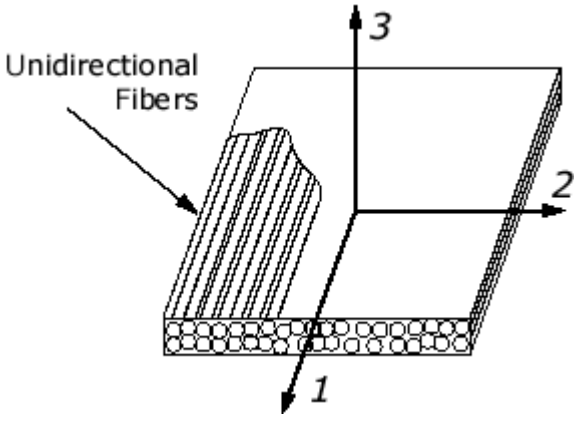

Figure 3: Orthogonal laminate with three main directions (eFunda, 2017)

In practice, when a lamina is considered in two-dimensional state of stress, Sutcliffe et al. simplifies the orthotropic stress-strain relationship to:

$$\begin{bmatrix} \varepsilon_1 \\ \varepsilon_2 \\ \gamma_{12} \end{bmatrix} = \begin{bmatrix} \frac{1}{E_1} & -\frac{v_{21}}{E_2} & 0 \\ -\frac{v_{12}}{E_1} & \frac{1}{E_2} & 0 \\ 0 & 0 & \frac{1}{G_{12}} \end{bmatrix} \begin{bmatrix} \sigma_1 \\ \sigma_2 \\ \tau_{12} \end{bmatrix} \quad 2.7$$

This equation is called the compliance matrix S, where $\varepsilon = S\sigma$. Taking the inverse of the compliance matrix, Sutcliffe et al. obtain the lamina stiffness matrix, $\sigma = Q\varepsilon$.:

$$\begin{bmatrix} \sigma_1 \\ \sigma_2 \\ \tau_{12} \end{bmatrix} = \begin{bmatrix} \frac{E_1}{1 - v_{12}v_{21}} & \frac{v_{12}E_2}{1 - v_{12}v_{21}} & 0 \\ \frac{v_{12}E_2}{1 - v_{12}v_{21}} & \frac{E_2}{1 - v_{12}v_{21}} & 0 \\ 0 & 0 & G_{12} \end{bmatrix} \begin{bmatrix} \varepsilon_1 \\ \varepsilon_2 \\ \gamma_{12} \end{bmatrix} \quad 2.8$$

where

$$Q = \begin{bmatrix} \frac{\mathrm{E_1}}{1 - \mathrm{v_{12}v_{21}}} & \frac{\mathrm{v_{12}E_2}}{1 - \mathrm{v_{12}v_{21}}} & 0 \\ \frac{\mathrm{v_{12}E_2}}{1 - \mathrm{v_{12}v_{21}}} & \frac{\mathrm{E_2}}{1 - \mathrm{v_{12}v_{21}}} & 0 \\ 0 & 0 & \mathrm{G_{12}} \end{bmatrix}$$

Here the stiffness matrix components are subscripted with Q_{ij} as stated below in equations 2.9-2.12.

$$Q_{11} = \frac{E_1}{1 - v_{12}v_{21}} \quad 2.9$$

$$Q_{12} = Q_{21} = \frac{v_{12}E_2}{1 - v_{12}v_{21}} \quad 2.10$$

$$Q_{22} = \frac{E_2}{1 - v_{12}v_{21}} \quad 2.11$$

$$Q_{66} = G_{12} \quad 2.12$$

Sutcliffe et al. mean that the Q-values are calculated using the elastic properties as inputs from chapter 2.3.1. These values describe the properties in determined directions with respect to direction 1, i.e. the stiffness component Q_{11} in direction 1 and Q_{22} in direction 2. However, considering an orthotropic lamina it is usually necessary to know the stress-strain relationships also in arbitrary, off-axis coordinates. As illustrated in *Figure 4*, if a unidirectional lamina is rotated by an angle θ prior to the 1-2 axes, new relationships are found.

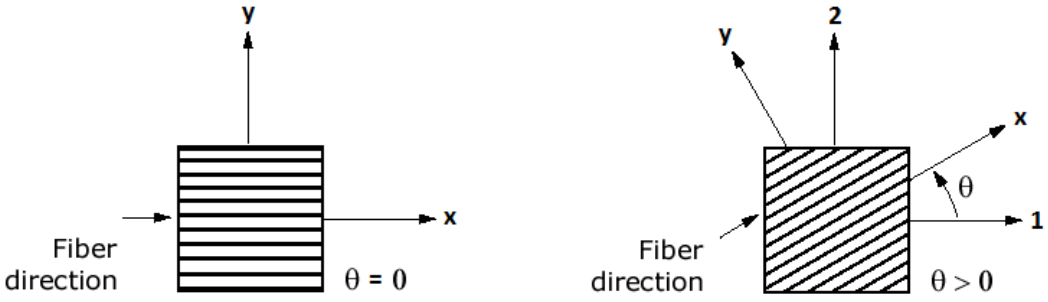

Figure 4: On-axis configuration for a UD lamina, where the x-axis is along the fiber and is in the longitudinal direction (left). If the lamina is rotated, an angle prior to the 1-2 axes is obtained (right). (Tsai & Hahn, 1980)

Hence, the new components yield:

$$\begin{bmatrix}\sigma_1\\ \sigma_2\\ \tau_{12}\end{bmatrix} = \begin{bmatrix}\overline{Q_{11}} & \overline{Q_{12}} & \overline{Q_{16}}\\ \overline{Q_{21}} & \overline{Q_{22}} & \overline{Q_{26}}\\ \overline{Q_{61}} & \overline{Q_{62}} & \overline{Q_{66}}\end{bmatrix}\begin{bmatrix}\varepsilon_1\\ \varepsilon_2\\ \gamma_{12}\end{bmatrix} \quad 2.13$$

where the $\overline{Q_{ij}}$ – values or "Qbars", which are the components of the transformed lamina stiffness matrix, Sutcliffe et al. define as follows:

$$\overline{Q_{11}} = c^4Q_{11} + 2c^2s^2(Q_{12} + 2Q_{66}) + s^4Q_{22} \quad 2.14$$

$$\overline{Q_{12}} = \overline{Q_{21}} = s^2c^2(Q_{11} + Q_{22} - 4Q_{66}) + (s^4 + c^4)Q_{12} \quad 2.15$$

$$\overline{Q_{16}} = \overline{Q_{61}} = sc[c^2(Q_{11} - Q_{12} - 2Q_{66}) + s^2(Q_{12} - Q_{22} + 2Q_{66})] \quad 2.16$$

$$\overline{Q_{22}} = s^4Q_{11} + 2c^2s^2(Q_{12} + 2Q_{66}) + c^4Q_{22} \quad 2.17$$

$$\overline{Q_{26}} = \overline{Q_{62}} = sc[s^2(Q_{11} - Q_{12} - 2Q_{66}) + c^2(Q_{12} - Q_{22} + 2Q_{66})] \quad 2.18$$

$$\overline{Q_{66}} = s^2c^2(Q_{11} - 2Q_{12} + Q_{22}) + (s^2 - c^2)^2Q_{66} \quad 2.19$$

with $s = \sin\theta$ and $c = \cos\theta$.

2.3.3 Analysis of a Laminate Using Plate Theory

Since $\bar{Q}$-values describe only the properties of a single lamina, a laminate must contain all the $\bar{Q}$-values for each layer. In other words, the stiffness of the laminate is the sum of the lamina stiffnesses (Verein Deutscher Ingenieure, 2006). A schematic for a laminate plate geometry with ply numbering system is shown in *Figure 5*.

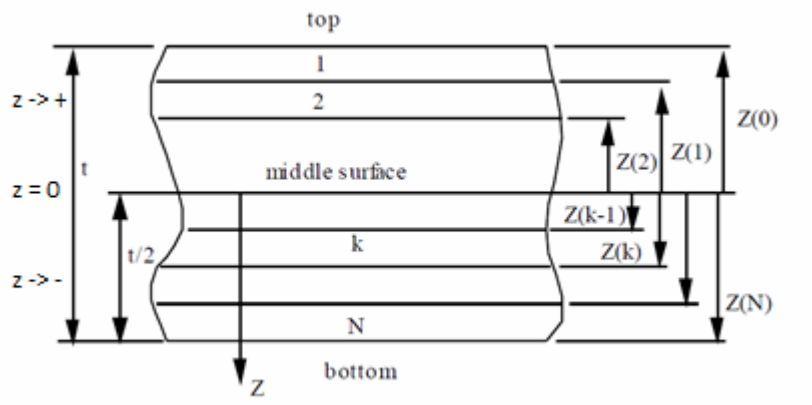

Figure 5: Plate geometry of a laminate with ply numbering system. (Sutcliffe, et al., 2013)

Forces and moments are used in the laminated plate analysis because of convenience (Sutcliffe, et al., 2013). The stress-strain relationship of the whole laminate becomes a 6x6 stiffness matrix system as shown in Eq. 2.20. The A-components represent the laminate extensional stiffness, B-components the coupling stiffness and D-components the bending stiffness, each forming their own sub-matrices. ε_i^o components are the strains on the middle surface and κ_i^o are the curvatures of the middle surface. Sutcliffe et al. explain that there is no coupling between in-plane and bending terms for a balanced symmetric laminate. Hence, the B sub-matrix is zero. In terms of unsymmetrical laminates coupling exists, indicating that the B-matrix is not zero.

$$\begin{Bmatrix} N_x \\ N_y \\ N_{xy} \\ M_x \\ M_y \\ M_{xy} \end{Bmatrix} = \begin{bmatrix} A_{11} & A_{12} & A_{16} & B_{11} & B_{12} & B_{16} \\ A_{12} & A_{22} & A_{26} & B_{12} & B_{22} & B_{26} \\ A_{16} & A_{26} & A_{66} & B_{16} & B_{26} & B_{66} \\ B_{11} & B_{12} & B_{16} & D_{11} & D_{12} & D_{16} \\ B_{12} & B_{22} & B_{26} & D_{12} & D_{22} & D_{26} \\ B_{16} & B_{26} & B_{66} & D_{16} & D_{26} & D_{66} \end{bmatrix} \begin{Bmatrix} \varepsilon_x^o \\ \varepsilon_y^o \\ \gamma_{xy}^o \\ \kappa_x \\ \kappa_y \\ \kappa_{xy} \end{Bmatrix} \quad 2.20$$

where

N_i = the force per unit length in the i:th direction

M_i = the moment per unit length

$A_{ij} = \sum \overline{Q_{ij}} t_k$, where t_k = layer thickness

$B_{ij} = \sum \overline{Q_{ij}} t_k z_k$, where z_k = distance from neutral line to outer surface of the k:th lamina

$D_{ij} = \sum \overline{Q_{ij}} (t_k z_k^2 + \frac{t_k^3}{12})$.

ε_i^o = strains on the middle surface

κ_i^o = curvatures of the middle surface

For simplicity, the stiffness matrix can be written as follows:

$$\begin{bmatrix} N \\ M \end{bmatrix} = \begin{bmatrix} A & B \\ B & D \end{bmatrix} \begin{bmatrix} \varepsilon \\ \kappa \end{bmatrix} \quad 2.21$$

For a symmetric laminate $B_{ij} = 0$, thus the inverse of the stiffness matrix gives the compliance matrix:

$$\begin{bmatrix} \varepsilon \\ \kappa \end{bmatrix} = \begin{bmatrix} A^{-1} & 0 \\ 0 & D^{-1} \end{bmatrix} \begin{bmatrix} N \\ M \end{bmatrix} \quad 2.22$$

which is used to calculate the stresses and strains of the laminate in conjunction with laminate loads. (Sutcliffe, et al., 2013)

2.3.4 In-Plane Behavior of a Symmetric Laminate

When manufacturing a laminate, the individual laminae are bonded securely together and when loaded they all experience the same strain. This means that the strains are independent of z-direction. However, the stresses will not be the same in each ply because all of them have different stiffness. Furthermore, the stiffness matrix [Q] is symmetric about its diagonal and it is necessary to use average stresses. This together with the independent strains, following stiffness matrix can be derived:

$$\begin{bmatrix} \sigma_X \\ \sigma_Y \\ \tau_{XY} \end{bmatrix} = \begin{bmatrix} A_{11} & A_{12} & A_{16} \\ A_{21} & A_{22} & A_{26} \\ A_{61} & A_{62} & A_{66} \end{bmatrix} \begin{bmatrix} \varepsilon_X \\ \varepsilon_Y \\ \gamma_{XY} \end{bmatrix} \tag{2.23}$$

where, for example

$$A_{11} = \sum \overline{Q_{11}}^{k} \left(\frac{2t_k}{t}\right) \tag{2.24}$$

where

t = thickness of laminate

t_k = thickness of k:th layer

$\overline{Q_{11}}^{k}$ = Qbar for k:th layer

For balanced angle-ply laminates and cross-ply laminates, the stiffness matrix can be simplified by the fact that $A_{16} = A_{61} = 0$ and $A_{26} = A_{62} = 0$. *Figure 6* shows the effect of A_{16} being unequal to zero.

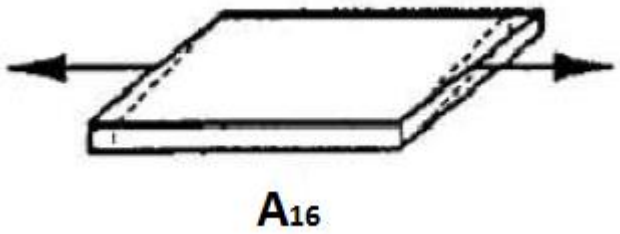

Figure 6: The effect of component A_{16} on the laminate. (Verein Deutscher Ingenieure, 2006)

Taking now the inverse of the A-matrix, the compliance matrix is obtained

$$\begin{bmatrix} \varepsilon_X \\ \varepsilon_Y \\ \gamma_{XY} \end{bmatrix} = \begin{bmatrix} A_{11} & A_{12} & 0 \\ A_{21} & A_{22} & 0 \\ 0 & 0 & A_{66} \end{bmatrix}^{-1} \begin{bmatrix} \sigma_X \\ \sigma_Y \\ \tau_{XY} \end{bmatrix} \quad 2.25$$

or it may be written

$$\begin{bmatrix} \varepsilon_X \\ \varepsilon_Y \\ \gamma_{XY} \end{bmatrix} = \begin{bmatrix} a_{11} & a_{12} & 0 \\ a_{21} & a_{22} & 0 \\ 0 & 0 & a_{66} \end{bmatrix} \begin{bmatrix} \sigma_X \\ \sigma_Y \\ \tau_{XY} \end{bmatrix} \quad 2.26$$

The laminate properties might then be calculated by

$$E_X = \frac{1}{a_{11}} \qquad E_Y = \frac{1}{a_{22}} \qquad G_{XY} = \frac{1}{a_{66}}$$

$$v_X = \frac{-a_{12}}{a_{11}} \qquad v_Y = \frac{-a_{12}}{a_{22}} \quad 2.27$$

where

$E_X =$ elastic modulus in the hoop direction (if direction 1 is set as hoop direction)

$E_Y =$ elastic modulus in the axial direction (if direction 2 is set as axial direction)

G_{XY} = in-plane shear modulus

$v_{X/Y}$ = Poisson's ratios (Benham, et al., 1996)

2.3.5 Thin-Walled Pressure Vessels

For determining the mechanical behavior of thin walled pressure vessels, a cylinder is defined below in *Figure 7*.

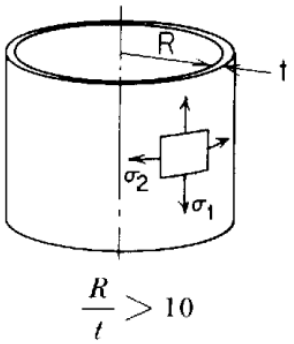

Figure 7: Cylinder with hoop and axial stresses, inner radius and thickness. (Young & Budynas, 2002).

The equations for axial stress σ_1 and hoop stress σ_2 yields:

$$\sigma_1 = \frac{pR}{2t} \qquad \sigma_2 = \frac{pR}{t} \qquad 2.28 \quad 2.29$$

where

R = inner radius of cylinder

p = unit pressure (force per unit area)

t = wall thickness (Young & Budynas, 2002)

The axial and hoop stresses are needed for calculating the strains or the internal pressure in the pipe (Benham, et al., 1996). Inserting equations 2.26 and 2.27 to the compliance matrix, equation 2.25, is giving

$$\begin{bmatrix} \varepsilon_X \\ \varepsilon_Y \\ \gamma_{XY} \end{bmatrix} = \begin{bmatrix} a_{11} & a_{12} & 0 \\ a_{21} & a_{22} & 0 \\ 0 & 0 & a_{66} \end{bmatrix} \begin{bmatrix} \frac{pR}{t} \\ \frac{pR}{2t} \\ \tau_{XY} \end{bmatrix} \qquad 2.30$$

Alternatively, internal pressure p may be taken outside the matrix, giving

$$\begin{bmatrix} \varepsilon_X \\ \varepsilon_Y \\ \gamma_{XY} \end{bmatrix} = \begin{bmatrix} a_{11} & a_{12} & 0 \\ a_{21} & a_{22} & 0 \\ 0 & 0 & a_{66} \end{bmatrix} \begin{bmatrix} \frac{R}{t} \\ \frac{R}{2t} \\ \tau_{XY} \end{bmatrix} p \qquad 2.31$$

Knowing the internal pressure and calculating for the hoop and axial strain, Benham et al. obtain

$$\varepsilon_X = p\left[a_{11}\left(\frac{R}{t}\right) + a_{12}\left(\frac{R}{2t}\right)\right] \qquad 2.32$$

$$\varepsilon_Y = p\left[a_{21}\left(\frac{R}{t}\right) + a_{22}\left(\frac{R}{2t}\right)\right] \qquad 2.33$$

3 METHOD

3.1 Pre-Investigation

Laminate plate theory states that in terms of in-plane behavior of a laminate, the elastic properties of the laminate can be calculated. All the $\bar{Q}$-values indicating the stiffness matrix of each single lamina, are multiplied by their thickness ratio with respect to the total thickness of the laminate. The products are summed up to obtain the stiffness matrix A. By taking the inverse, the compliance matrix with its a-components are obtained. However, the calculation model is valid only if $a_{16} = a_{61} = 0$ and $a_{26} = a_{62} = 0$. This indicates that the laminate has a constant thickness, hence balanced and no shear forces exist between the layers when pressure is applied. If there would be variations within the thickness of each layer, the laminate would not be balanced and shear forces would exist. Hence, the a-components above are unequal zero and would affect negatively on the elastic moduli, i.e. performance of the laminate. In this thesis, the possible variations within the thickness are investigated. The pre-investigation considered checking out the stress distribution in a pipe wall when a perpendicular load is applied. Also, a sample of PN10 DN300 pipe from River Plast Oy was machined and prepared for microscope analysis to investigate the possible variation within the thickness of the single laminae.

3.1.1 Von Mises Stress Distribution

In order to figure out the stacking order of the material combinations it was studied how stresses are distributed within the thickness of a pipe when an inner pressure is induced. By the result obtained from this, it can be roughly stated where the axial reinforcements are most preferable to be located within the support. This statement was induced quickly by use of COMSOL Multiphysics 5.1. The rectangle in *Figure 5* represents an arbitrary cross-section of a pipe wall with fixed top and bottom edges. A pressure is induced from the left hand side so that the distribution of the von Mises stress can be seen within the wall thickness. Von Mises stress refers to distortion energy theory, indicating that "a ductile solid will yield when the distortion energy density reaches a critical value for that material" (UFL MAE, 2017). Alternatively, the maximum principal stress theory may have been applied because it can be only used for brittle materials. The theory states that

the material fails when the stress in the specimen reaches a critical value in the material. From *Figure 8*, it can be stated that the stresses increase towards the inner surface. Hence, it is preferable to stack the axial reinforcements at the inner layers of the support.

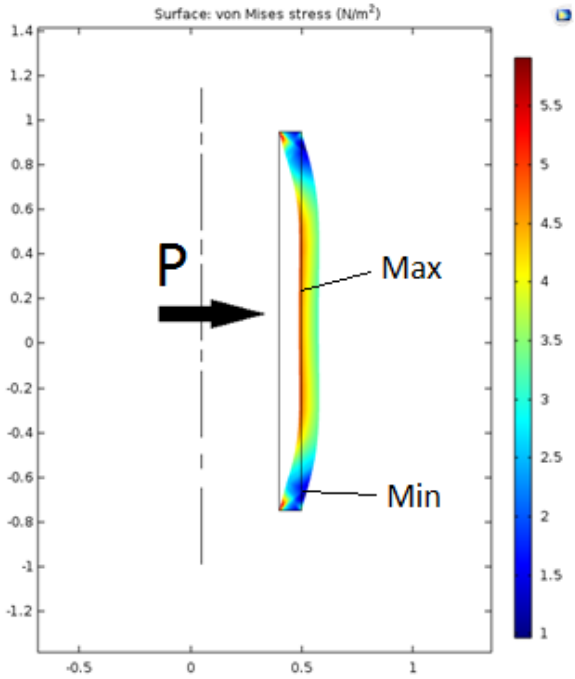

Figure 8: Stress distribution in a cross-section of a pipe wall with fixed ends. A force is applied from the inside and the results indicate that the stresses are highest at the inner surface. (Tony Lallinaho)

3.1.2 Machining the Sample Pipe

A 30 cm long sample of the pipe PN10 DN300 currently being manufactured was delivered from River Plast Oy to Arcada in order to be analyzed. The purpose was to compare possible variations in thickness of each layer along the circumference. This meant that the circumference was divided in 10 equal pieces, each 36 degrees (360/10) as illustrated in *Figure 9*.

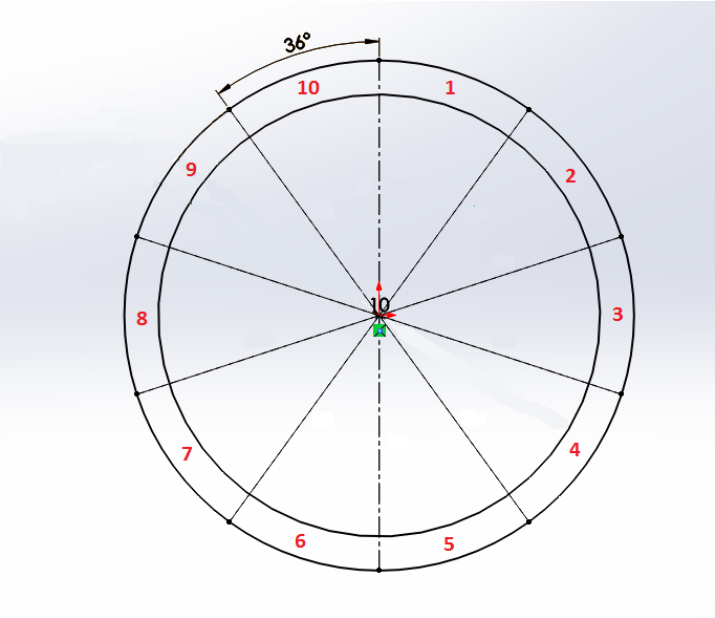

Figure 9: The circumference was divided in 10 equal segments, each 36 degrees (Tony Lallinaho)

The cutting operation was done by milling 20 mm deep slots from the top of the cylinder. Furthermore, a slot mill was used to create a 16 mm thick cut-out ring, as it can be seen on the left hand side in *Figure 10*. This way all the 10 samples were directly cut out from the cylinder (on the right hand side), following by wet polishing the cross-sections from number 320 up to 4000.

Figure 10: The 16 mm thick samples (to right) were milled with a slot mill in the HAAS milling machine (to left) at Arcada lab. (Tony Lallinaho)

3.1.3 The Microscope

Each sample was investigated with a microscope at the Arcada chemistry lab. The purpose was to measure the variation in the thickness of each layer around the circumference of the pipe. It was expected and by the pictures also verified that the support layer consisted of 6 layers of 2400 Tex roving and 3 layers of woven UD fabric (420 g/m^2), totally 9 laminae. The term 'Tex' is defined as "Weight in grams per kilometer (1,000 meters) of yarn, fiber, filament or strands" (Owens Corning, 2017). The laminae were stacked in the following sequence beginning from the inner layers:

Roving – roving – roving – axial – roving – axial – roving – axial – roving.

Because only 3 layers fitted in one picture, 3 pictures of each sample were needed to get all the 9 layers recorded. Each sample was measured from the middle of the cross-section. By a calibration tool for 5x zoom on the microscope, the pixels obtained from Gimp 2.0 was converted to micrometers. Gimp 2.0 is an open-source raster graphics editor, which allows the user to create and edit images. The measurements were marked on the pictures, as it can be seen in an example from sample number 9 in *Figure 11*. Representing the last 3 layers of the support, the red line highlights the thickness of the woven roving layer and the blue corresponds to the axial layer. In the latter, the fibers are straightly pointed towards the camera, i.e. the fibers are aligned perpendicular to the pipe circumference. The dark spots inside the axial fiber bundles are empty slots indicating that the bundle has not been impregnated completely, hence the dry fibers are adhering to the surrounding, impregnated fibers. Above the last roving layer the dark bulk area is the surface layer. *Figure 12* shows the 3 first roving layers of sample number 5. Here, the interfaces between the layers can easily be distinguished due to alternating winding direction.

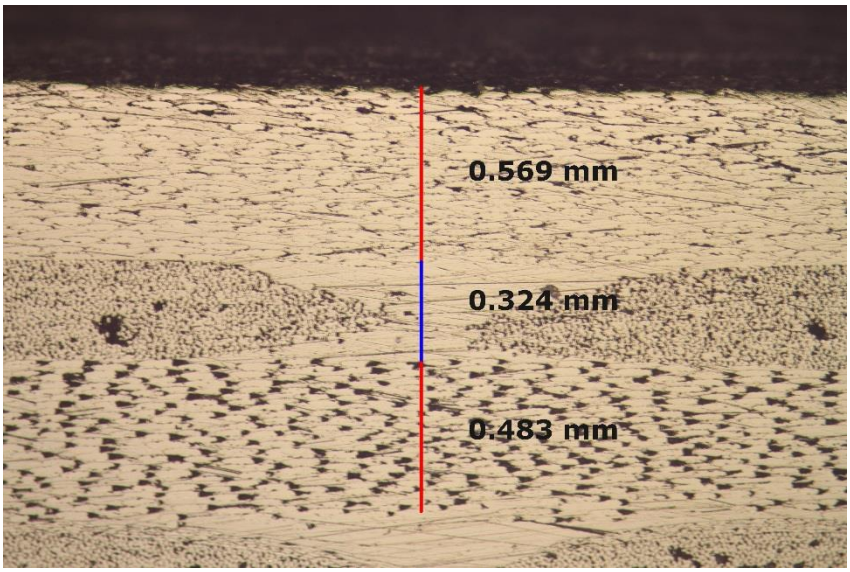

Figure 11: Cross-section with 5x zoom of the last three layers within the support of sample number 9. Measurements of the roving thickness (red) and axial thickness (blue) were calculated with the aid of calibration tools and Gimp 2.0 (Tony Lallinaho)

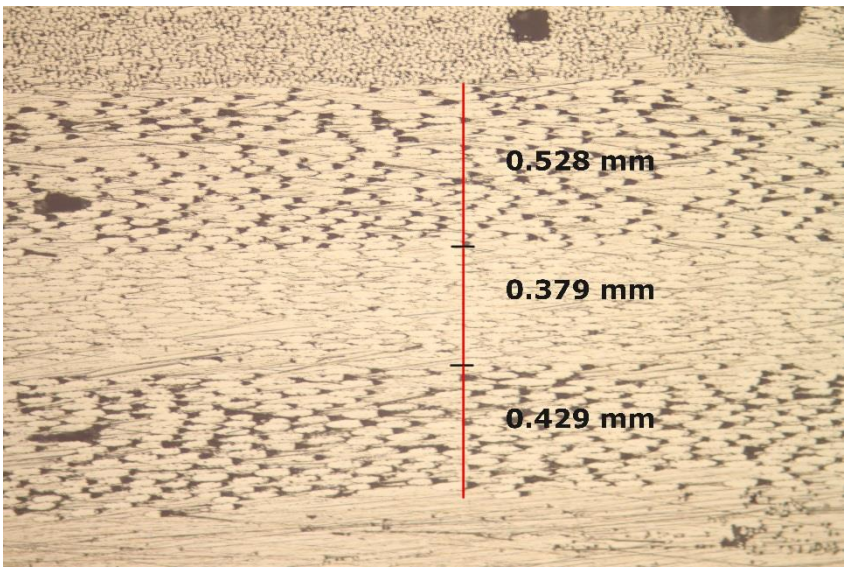

Figure 12: The 3 first roving layers can easily be distinguished because of alternating winding direction. The picture is taken from sample number 5 (Tony Lallinaho)

It turned out that there is way more variation within the support layer than that in the entire support thickness (4.5%) and wall thickness (2.7%). An overview of the thickness distribution within the support layer is presented in *Table 1*.

Table 1: Thickness distribution of each layer in the support around the circumference at an arbitrary point. There is more or less variation within the support. On the other hand, the variation in the entire thickness of each sample is significantly less (2.7 %).

sample #	t1	t2	t3	t4	t5	t6	t7	t8	t9	t_tuki	t_tot	*unit*
1	556.6474	455.4913	476.8786	432.3699	468.2081	383.815	464.1618	311.5607	390.7514	3939.88	7650	*µm*
2	575.1445	365.896	540.4624	336.9942	489.5954	368.7861	413.2948	457.8035	476.8786	4024.86	7660	*µm*
3	550.289	406.9364	480.9249	353.1792	563.0058	311.5607	515.0289	520.8092	508.6705	4210.4	7670	*µm*
4	657.8035	349.711	448.5549	320.8092	495.9538	378.6127	391.3295	543.9306	438.7283	4025.43	7850	*µm*
5	613.8728	330.6358	483.237	368.7861	435.8382	391.3295	527.7457	378.6127	429.4798	3959.54	7450	*µm*
6	566.474	343.3526	461.2717	406.9364	479.7688	359.5376	483.237	406.9364	632.948	4140.46	7700	*µm*
7	635.8382	334.104	454.9133	334.104	553.1792	353.1792	597.6879	610.4046	435.8382	4309.25	7850	*µm*
8	531.2139	365.3179	540.4624	358.9595	483.237	362.4277	486.1272	362.4277	493.0636	3983.24	7650	*µm*
9	569.3642	324.2775	483.237	397.1098	451.4451	416.185	445.0867	447.9769	495.9538	4030.64	7550	*µm*
10	521.3873	620.2312	473.9884	327.1676	489.5954	635.8382	416.763	470.5202	559.5376	4515.03	8200	*µm*
t(avg)	577.8035	389.5954	484.3931	363.6416	490.9827	396.1272	474.0462	451.0983	486.185	4113.87	7723	*µm*
std_dev	44.51426	90.39299	31.89392	37.45146	39.99009	88.54568	62.21058	90.56951	70.52573	183.471	206	*µm*
variation	**7.7**	**23.2**	**6.6**	**10.3**	**8.1**	**22.4**	**13.1**	**20.1**	**14.5**	**4.5**	**2.7**	*%*

roving
2400 Tex roving
axial
UD weave 420 g/m2
Material
E-glass

It can be observed that the magnitude of variation is alternating between the even and the odd layers. An illustration of this can be observed in *Figure 13* showing that the variation is significantly higher in the even layers than those in the odd.

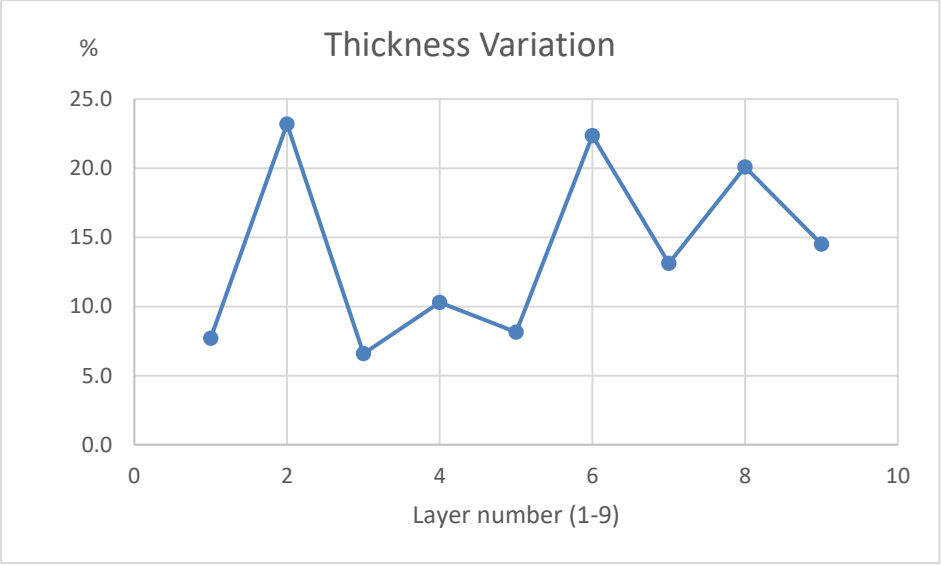

Figure 13: Thickness variation as a function of layer number (Tony Lallinaho)

Also, the figure shows that the variation is quite the same within the inner layers (7-9) than those towards the outer section (1-6). The reason to the variation is unknown, but it can have to do with the alternating winding direction. However, it is to be remembered

that the data is taken from an arbitrary cross section of the pipe, thus it can't be stated that the distribution is the same along the entire length. This can be proven based on *Figure 14*, where the changing thickness can be seen clearly.

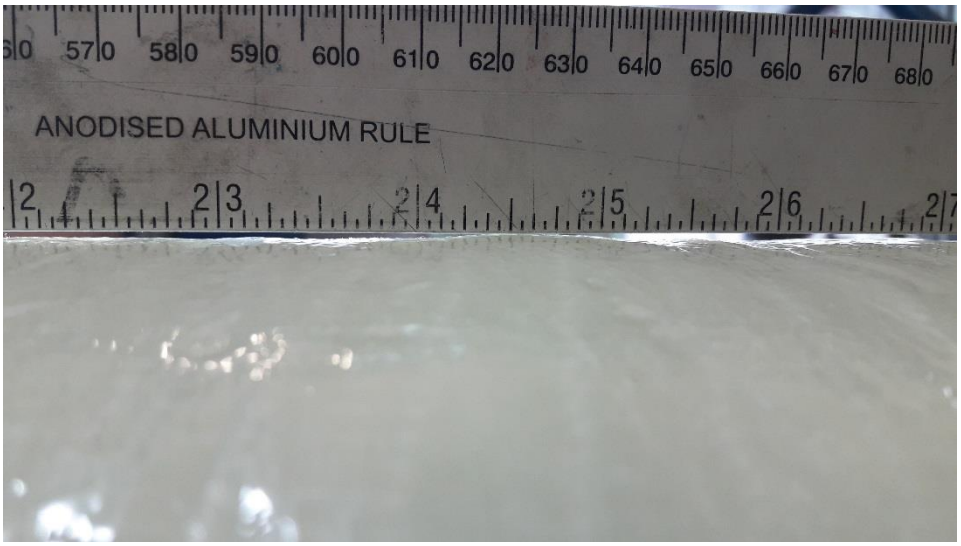

Figure 14: The thickness of the pipe is varying remarkably along its length, which indicates that the thickness distribution may also vary at different cross-sections. (Tony Lallinaho)

3.2 Determining the Inputs

As a starting point, the wall thickness boundaries were defined to obtain a minimum thickness that the support layer should not fall below. The elastic properties of the raw materials, including e.g. the elastic and shear modulus of the glass fiber and the resin, respectively, were determined. The entire analysis of the different stacking combinations was done by implementing the equations from classic lamina theory to Excel. The calculator was built up so that each layer type – hoop, axial and biaxial – had an own $\bar{Q}$-calculator, making them independent of each other. By this way, the elastic properties, the layer thickness and the $\bar{Q}$-values could be determined separately for each layer type. These values were then combined, giving the complete laminate thickness and a complete laminate stiffness matrix A to be converted into compliance matrix a. From this matrix, the elastic moduli were calculated both for the hoop and axial directions prior to eq. 2.25.

3.2.1 Parameters and Variables

The entire barrier section of the pipe was defined by the SFS 5162 standard and its thickness was determined constant, 2.36 mm. According to SFS 5166, the total thickness of pipe PN10 DN300 should not be less than 5 mm. This indicates that the support should be designed close to 2.64 mm, (5 – 2.36) so that it maintains six times the nominal pressure, i.e. 60 bar. This 2.64 mm optimum includes also the outer surface, but is neglected in the calculations since it's so thin.

Having the nominal diameter 300 mm and the optimal thickness 5 mm, the outer radius is then 155 mm. The calculations are simplified as the engineering constants of the barrier layer is neglected, meaning that the inner radius R in eq. 2.26 and 2.27 is defined as the radius up to the interface between the barrier and the support, hence $R = 152.36$ mm. Furthermore, the wall thickness t in eq. 2.26 and 2.27 becomes the thickness of the support. This remains variable until the support constructions are desired. A visualization of this is presented in *Figure 15*.

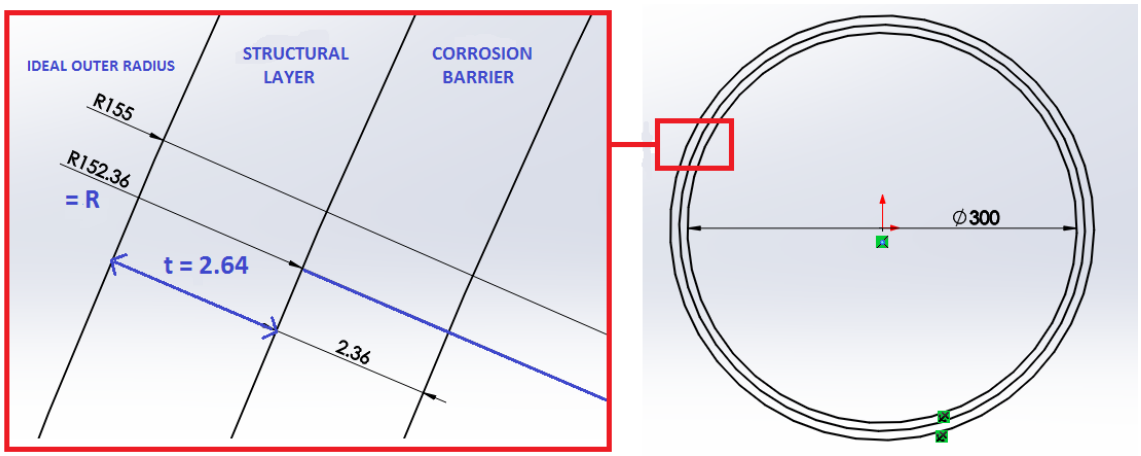

Figure 15: The inner radius "R" is defined as the radius up to the interface between the barrier and the support, hence R=152.36 mm. This makes "t" the support thickness, which is to be designed close to 2.64 mm. (Tony Lallinaho)

The classic lamina theory is applied to the strength calculations so that the arbitrary angle, θ from Eqs 2.13–2.19, corresponds to the winding angle α. The reference axis for the winding angle was determined to be the hoop direction with its modulus E_1, making E_2 the modulus in axial direction, respectively. *Figure 16* shows this statement.

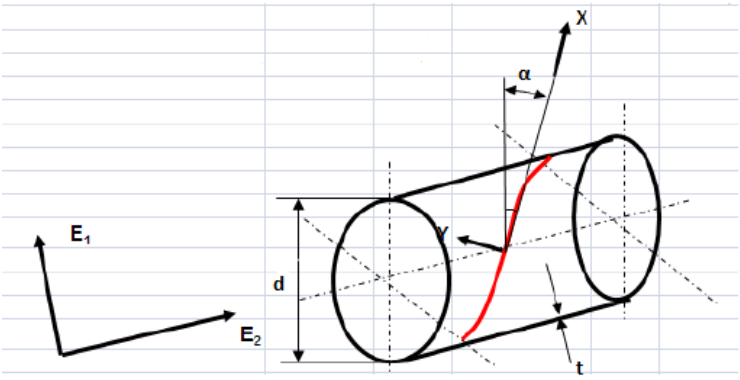

Figure 16: Definition of the pipe with the elastic moduli in the hoop (1) and axial (2) directions, inner diameter d, thickness t and winding angle α (Oy Scan Fibre Ltd, 2017)

Too much material in either hoop or axial direction would cause the material to become over strained in the other direction first. Least material is invested into the wall shell if strains rise in both hoop and axial direction simultaneously. It means that the strains in hoop and axial directions should remain equal at all pressures, thus

$$\varepsilon_{hoop} = \varepsilon_{axial} \tag{3.1}$$

$$a_{11} + \frac{a_{12}}{2} = a_{21} + \frac{a_{22}}{2} \tag{3.2}$$

By the fact that $a_{12} = a_{21}$, the optimal relationship yields

$$a_{11} = \frac{1}{2}(a_{22} + a_{12}) \tag{3.3}$$

Inserting Eq. 2.27, the relationship becomes

$$E_x = E_y(2 + v_x) \tag{3.4}$$

By having this as a design goal, the calculator is introduced in the following chapter.

3.2.2 The Calculator

By having the elastic properties of the raw materials taken from their technical data sheets, the $\bar{Q}$-values were calculated for each layer type incl. hoop, axial and biaxial variables.

In this thesis, the calculator is only tested so the material inputs are not necessarily correct. Also, some of the material types are only suggestions, which means that there is no guarantee that they can be applied in filament winding. By calculating the thickness ratio of each layer type according to Eq. 2.24 and multiplying by its own $\bar{Q}$-values, respectively, the complete stiffness matrix *A* was obtained. Assuming that $A_{16} = A_{61} = 0$ and $A_{26} = A_{62} = 0$ and taking the inverse of this giving the laminate compliance matrix *a*, the laminate's elastic properties could be calculated (see appendix A). Totally three different combinations were suggested and analyzed to calculate their elastic properties and strains in the required pressure (60 bar = 0.006 GPa, see appendix B and C). The first combination consisted completely of a 0/90 biaxial stich, including 80% of fibers in roll length direction and 20% in the perpendicular direction. The suggestion for alternative 2 included 8 layers of 1200 Tex single-end roving (with winding angle 10.8°) and 2 layers of UD axial weave (300 g/m^2). The third combination was suggested with 4 layers of 2400 Tex single-end roving (winding angle 10.8°) and 3 layers of 0/90 biaxial stich. All the combinations were aimed to be designed so that their total thickness reached as close as possible to 2.64 mm. Fiber volume fraction was assumed to be 40 – 43%.

3.3 Design Improvements

It was stated that for balanced angle-ply laminates, the stiffness matrix can be simplified by the fact that $A_{16} = A_{61} = 0$ and $A_{26} = A_{62} = 0$. If so, the expansion of the circumference and the axial compression of the pipe is uniform when exposed to inner pressure. However, the variations found within the thickness cause the pipe to deform unevenly, indicating that the components cannot be zero. If the variations were minimized, the theoretical strength calculations would become more trustworthy, hence the laminate quality improved. This could be achieved by selecting a tape instead of using single end roving because the tape would contribute to more uniform laminae than the roving bundles. If single end roving is still used, the 1200 Tex roving could be preferred instead of 2400 Tex based on the failure mode theory, where it was stated that a macroscopic crack in a lamina will extend through the entire layer up to the interface of the neighboring layers. In practice, this means that the more layers a laminate consists of, the more likely the whole laminate will not break at the same area. The effect could be improved by stacking

the laminate so that the fiber orientation of each laminae is perpendicular to the neighboring layers. The axials could be wound earlier, i.e. closer to the interface to the corrosion barrier due to higher stresses. Instead of using glass fiber, basalt fibers could be considered as an option – in addition to better mechanical properties, the material is compatible with vinyl ester resin and is not that much more expensive than glass fiber in big volumes.

4 RESULTS

The calculation tool for dimensioning was successfully implemented and tested with three different stacking combinations for the support, each giving their own strains in the main directions. On the other hand, it should be studied separately if the laminates are capable to withstand these strains without failing. The thickness of these combinations was aimed to correspond the optimal support thickness 2.64 mm, which in turn was defined based on the corrosion barrier. On the other hand, it was found out that the calculation model has shortages, which contribute to higher elastic properties than the laminate will have in practice. It assumes that the wall thickness is constant, which is wrong because it was found out that there is variation. Also, the applied calculation model is limited to the middle section of the pipe ignoring the fixed ends, where the stress-strain behavior is different (see *Figure 8*). When it comes to pipe dimensions, the model is valid only if the radius-to-thickness ratio is higher than 10, as indicated in *Figure 7*.

5 DISCUSSION

Since it was found that there are remarkable thickness variations along the length of the pipe, it would be recommended to make cutouts of a thicker cross-section and inspect the layers also from the hoop direction. This would give data of the thickness variation within the layers in the length direction. For further studies, it would be considerable to measure the change in the pipe dimensions at different sections – both in hoop and axial directions – during pressure testing. In the first case, the pipe could be surrounded by a ring of a larger diameter than the outer diameter of the pipe. Before applying pressure, the initial distance between the ring and the pipe could be measured at different points across the circumference. When pressure is applied, the change in distance could be recorded. The idea is represented in *Figure 17*.

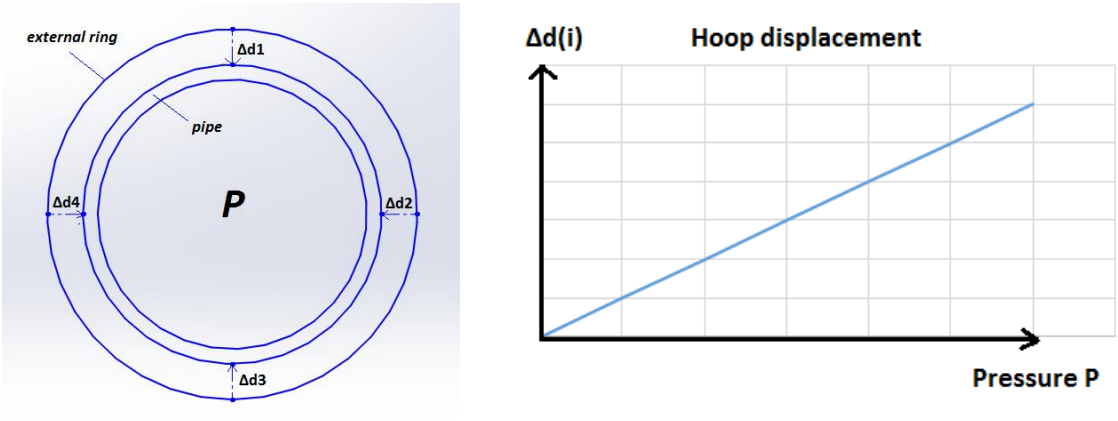

Figure 17: The distance between the ring and the pipe could be measured across the circumference and the change in distance recorded in a graph for each point. (Tony Lallinaho)

In the case regarding the axial direction, a laser could be introduced to record the change in distance between the pipe surface and the laser beam at different cross-sections, as seen in *Figure 18*.

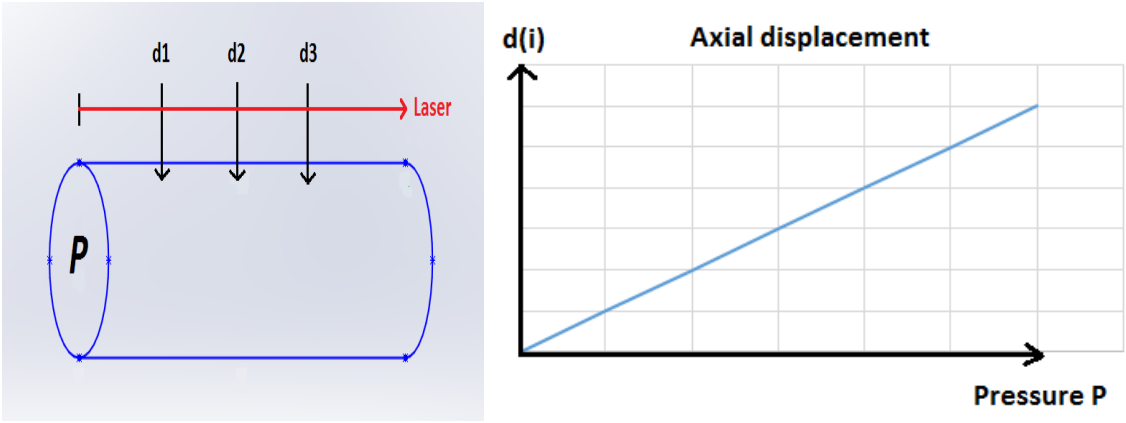

Figure 18: When applying pressure, a laser beam could be used to record the expansion of the pipe at different cross-sections. (Tony Lallinaho)

6 CONCLUSION

The minimum thickness for the support structure of PN10 DN300 pipe was defined. It turned out that the implementation of the formulas from the lamina theory for dimensioning a pressure vessel was successfully made in Excel. The calculator considered all the formulas from the single, unidirectional layer properties via single lamina properties to the complete laminate stiffness and compliance matrices. From the compliance matrix,

the elastic properties of the laminate could be calculated and used to estimate the strains in the pressure vessel when an inner pressure is applied. However, there are some shortages in the calculator. The calculator is modelled relying on a theory that considers only the middle section of the pipe and assumes that the components A_{16}, A_{61}, A_{26} and A_{62} in the laminate matrix system are zero, meaning that there are no shear forces between the layers and the thickness is constant. It turned out that there are variations within the thickness, indicating contradictions with the statements in the theory. Based on these and the other shortages, it can be concluded that the calculator provides too high moduli. Design improvements to winding strategy were suggested for example by that a tape could be used instead of roving. In addition, further research of the pipe is recommended so that its behavior can be interpreted better during pressure testing. Based on the remarkable amount of suggestions and assumptions, this thesis would work as a good reference for further studies in the field of filament wound GRP process pipes.

REFERENCES

Benham, P., Crawford, R. & CG, A., 1996. *Mechanics of Engineering Materials.* 2nd toim. Singapore: Longman Group.

eFunda, 2017. *Lamina Stress-Strain Relations for Principal Directions.* [Online] Available at: http://www.efunda.com/formulae/solid_mechanics/composites/comp_lamina_principal.cfm [Accessed 8 March 2017].

Mutasher, S., Mir-Nasiri, N. & Lee, C. L., 2012. Small-Scale Filament Winding Machine For Producing Fiber Composite Products. *Journal of Engineering Science and Technology*, Osa/vuosikerta VII, pp. 156-168.

Owens Corning, 2017. *Composite Solutions Guide.* [Online] Available at: http://composites.owenscorning.com/pdf/rft-guide/Composite_Solutions_Guide_page119-125.pdf [Accessed 5 May 2017].

Oy Scan Fibre Ltd, 2017. *Paineputken suunnittelu NP10 NS300,* s.l.: s.n.

Plasticon Composites, 2017. *Piping Systems.* [Online] Available at: http://www.plasticoncomposites.com/media/download/0001/01/17fa6f981626b8a46de6eed3545a12512d9c10a8.pdf [Accessed 14 April 2017].

Prof. Dr. Tapavicza, M. v., 2010. *Introduction to Fiber Composite Materials,* s.l.: s.n.

Rafiee, R., 2013. Apparent Hoop Tensile Strength Prediction of Glass Fiber-Reinforced Polyester Pipes. *Journal of Composite Materials,* 47(11), pp. 1377-1386.

Rafiee, R., 2013. Experimental and theoretical investigations on the failure of filament wound GRP pipes. *Composites Part B Engineering,* 450(1), pp. 257-267.

Roylance, D., 2000. *Laminated Composite Plates,* Cambridge: s.n.

Saarela, O., Airasmaa, I., Kokko, J. & Skrifvars, M., 2003. *Komposiittirakenteet.* 2nd toim. Helsinki: Muoviyhdistys ry.

Sutcliffe, M. P. F., Xin, X. J., Fleck, N. A. & Curtis, P. T., 2013. *Composite Compressive Strength Modeller - A Windows™ based composite design tool for engineeers, Version 2.0,* Cambridge: s.n.

Tsai, S. W. & Hahn, H. T., 1980. *Introduction to Composite Materials.* Lancaster(Pennsylvania): Technomic Publishing Company.

UFL MAE, 2017. *EML4500 Finite Element Analysis and Design.* [Online] Available at: http://web.mae.ufl.edu/nkim/eas4200c/VonMisesCriterion.pdf [Accessed 15 May 2017].

Verein Deutscher Ingenieure, 2006. *Guideline VDI 2014 Part 3 : Development of Fibre-Reinforced Plastics Components Analysis.* Düsseldorf: s.n.

Young, W. C. & Budynas, R. G., 2002. *Roark's Formulas for Stress and Strain,* s.l.: McGraw-Hill Companies.

APPENDICES

Appendix A

Hoop (1)			**Stiffness**		
Q_11	29.85432	GPa	A11	24.90579499	
Q_12=Q_21	2.241812	GPa	A12	2.062798701	
Q_16=Q_61	4.706	GPa	A16	3.764799829	
Q_22	5.149568	GPa	A22	10.45611959	
Q_26=Q_62	0.184652	GPa	A26	0.147721716	
Q_66	2.81532	GPa	A66	2.636307451	
Axial (2)			**Compliance**		
Q_11	5.11169	GPa	a11	0.040818254	
Q_12=Q_21	1.346747	GPa	a12	-0.00805269	
Q_16=Q_61	4.63E-18	GPa	a16	0	
Q_22	31.68233	GPa	a22	0.097226419	
Q_26=Q_62	1.83E-15	GPa	a26	0	
Q_66	1.920256	GPa	a66	0.379318429	
Biaxial (3)			**A-Matrix**		
Q_11	31.41418	GPa	24.905795	2.062798701	0
Q_11	5.081716	GPa	2.0627987	10.45611959	0
Q_12=Q_21	1.341573	GPa	0	0	2.636307
Q_12=Q_21	1.341573	GPa			
Q_16=Q_61	0	GPa	**a-Matrix**		
Q_16=Q_61	4.74E-18	GPa	0.0408183	-0.00805269	0
Q_22	5.081716	GPa	-0.008053	0.097226419	0
Q_22	31.41418	GPa	0	0	0.379318
Q_26=Q_62	0	GPa			
Q_26=Q_62	1.81E-15	GPa	**E(1)_hoop**	24.49884302	GPa
Q_66	1.908764	GPa	**E(2)_axial**	10.28527026	GPa
Q_66	1.908764	GPa	**G12**	2.636307451	GPa
			V1	0.197281476	
Thickness ratio			**V2**	0.082824046	
n1	0.8				
n2	0.2				
n3	0				

Appendix B

Stack number-->	1	2	3
m_h(oop) (g/m2)	-	2132	2132
m_a(xial) (g/m2)	-	600	0
m_b(iax) (g/m2)	3000	0	600
fiber volume	0.403827	h:0.435, a:0.4	h:0.435, b:0.4
t_h (mm)	0.233981851	0.241198298	0.482396597
t_a (mm)	0.058495463	0.295275591	
t_b (mm)	0	0	0.196850394
t_tot_h (mm)	**2.339818511**	**1.929586388**	**1.929586388**
t_tot_a (mm)	**0.584954628**	**0.590551181**	**0**
t_tot_b (mm)	**0**	**0**	**0.590551181**
n_h	0.8	0.765667086	0.765667086
n_a	0.2	0.234332914	0
n_b	0	0	0.234332914
Q_h11	29.85432123	31.90505195	31.90505195
Q_h12	2.241811518	2.352804086	2.352804086
Q_h16	4.705999786	5.050789045	5.050789045
Q_h22	5.149567722	5.409367208	5.409367208
Q_h26	0.184652145	0.217154103	0.217154103
Q_h66	2.815320268	2.980676668	2.980676668
Q_a11	5.111690055	5.081715919	0
Q_a12	1.346747433	1.341573003	0
Q_a16	4.62921E-18	4.7404E-18	0
Q_a22	31.68232706	31.41417527	0
Q_a26	1.826E-15	1.80983E-15	0
Q_a66	1.920256183	1.908763951	0
Q_b11	0	0	31.41417527
Q_b11	0	0	5.081715919
Q_b12=Q_b21	0	0	1.341573003
Q_b12=Q_b21	0	0	1.341573003
Q_b16=Q_b61	0	0	0
Q_b16=Q_b61	0	0	4.7404E-18
Q_b22	0	0	5.081715919
Q_b22	0	0	31.41417527
Q_b26=Q_b62	0	0	0
Q_b26=Q_b62	0	0	1.80983E-15
Q_b66	0	0	1.908763951
Q_b66	0	0	1.908763951
A_11	24.90579499	25.73568466	28.70474242
A_12	2.062798701	2.120220937	2.115839359
A_16	3.764799829	3.889107564	3.867222928
A_22	10.45611959	11.39047306	8.417868698

A_26	0.147721716	0.16720866	0.166267749
A_66	2.636307451	2.734136743	2.953135347
a_11	0.040818254	0.0394617	0.035495073
a_12	-0.008052685	-0.007345395	-0.008921721
a_16	0	0	0
a_22	0.097226419	0.089159937	0.121037398
a_26	0	0	0
a_66	0.379318429	0.365746155	0.338623152
E(1) hoop (GPa)	**24.49884302**	**25.34102706**	**28.17292417**
E(2) axial (GPa)	**10.28527026**	**11.21579977**	**8.261909235**
G(12) (GPa)	**2.636307451**	**2.734136743**	**2.953135347**
V1	0.197281476	0.186139849	0.251350958
V2	0.082824046	0.082384478	0.073710446
support (in->out)	b x 10	r,r,a,r,a,r,r,r,r,r	r,b,r,b,r,b,r
material_h	-	1200 Tex	2400 Tex
material_a	-	UD 300 g/m2	-
material_b	stich warp:80,weft:20	-	biax (0/90) 200 g/m2
t_barrier (mm)	2.36	2.36	2.36
t_support (mm)	2.947773139	2.543137569	2.543137569
t_tot (mm)	**5.307773139**	**4.903137569**	**4.903137569**
w_angle_h (deg)	10.8	10.8	10.8
fiber bundles_h	0	40	40

Appendix C

Stack number-->	1	2	3	*Unit*
R	152.36	152.36	152.36	*mm*
t	2.947773139	2.543137569	2.543137569	*mm*
p	0.006	0.006	0.006	*GPa*
a_11	0.040818254	0.0394617	0.035495073	-
a_12 = a_21	-0.008052685	-0.007345395	-0.008921721	-
a_22	0.097226419	0.089159937	0.121037398	-
E(1)_h	24.49884302	25.34102706	28.17292417	*GPa*
E(2)_a	10.28527026	11.21579977	8.261909235	*GPa*
σ(1)_h	0.155059422	0.179730741	0.179730741	*GPa*
σ(2)_a	0.310118845	0.359461482	0.359461482	*GPa*
ε(1)_hoop	**1.140986508**	**1.286476789**	**1.115560402**	***%***
ε(2)_axial	**1.257858299**	**1.338439498**	**1.854712619**	***%***